Mechanisms and Instrument Electronics for the Ohio State Multi-Object Spectrograph (OSMOS)

R. Stoll, P. Martini, M. A. Derwent, R. Gonzalez, T. P. O'Brien, D. P. Pappalardo, R. W. Pogge, M.-H. Wong, R. Zhelem

Department of Astronomy, The Ohio State University, 140 W 18th Ave, Columbus, OH 43210, USA

ABSTRACT

The Ohio State Multi-Object Spectrograph (OSMOS) is a new facility imager and spectrograph for the 2.4m Hiltner telescope at the MDM Observatory. We present a detailed description of the mechanical and electronic solutions employed in OSMOS, many of which have been developed and extensively tested in a large number of instruments built at Ohio State over the past ten years. These solutions include robust aperture wheel and linear stage designs, mechanism control with MicroLYNX programmable logic controllers, and WAGO fieldbus I/O modules.

1. INTRODUCTION

The Ohio State Multi-Object Spectrograph (OSMOS) is a new facility instrument for the 2.4m Hiltner telescope at the MDM Observatory. It was commissioned in April 2010. OSMOS has a 20' diameter FOV with 0.3"/pixel when used with the MDM 4K detector, which is a 4064x4064 CCD with 15μm pixels. The instrument is an all-refractive design with no folds and may be used either as an imager or as a spectrograph. This design produces good image quality and sensitivity from approximately 350–1000nm. The present disperser complement includes a very low-resolution triple prism that covers this entire wavelength range and a low-resolution volume-phase holographic (VPH) grism with maximum efficiency at 450nm. These dispersers produce resolutions of 400–60 and 1600, respectively, for a 1" slit.

OSMOS has four six-aperture wheel mechanisms: a slit wheel, a disperser wheel, and two filter wheels. This allows up to five dispersers, five longslits or multi-object slit masks, and ten filters to be loaded in the instrument at any time. These wheels may be reconfigured in only a few seconds, which facilitates rapid spectrographic acquisitions, target-of-opportunity science, and queue-scheduled observations. The slit wheel and two filter wheels are also readily accessible for configuration changes. Complete details of OSMOS will be presented separately.[1]

OSMOS adds a new, multi-object capability to MDM. It was designed to employ VPH gratings, which are more efficient than ruled gratings. The wavelength range over which OSMOS performs well is wider than that of the facility long-slit spectrograph at MDM, which is the Boller & Chivens CCD Spectrograph (CCDS). In the blue, this is primarily due to the greater efficiency of the dispersers. In the red, it is due to the optical design. Unlike CCDS, OSMOS was designed to operate over nearly the entire wavelength range accessible with CCDs from ground-based observatories. This advantage will soon be enhanced, as we plan to develop a red-sensitive detector in the next year. In addition, the OSMOS long slits may be up to 20' in length, compared to the 5.2' length of CCDS at the 2.4m telescope.

Several of these advantages are evident in some sample data from the OSMOS commissioning observations. The good image quality of OSMOS is evident from Fig. 1, an hour-long narrow-band (15Å) Hα exposure of the extended star formation disk of NGC 4625. The red efficiency of OSMOS and the low-resolution triple prism is shown in Fig. 2, a spectrum of the z=6.4 QSO discovered by Fan et al.[2] Although the spectrum shown is a sum of 40 minutes of observation, it was easily identifiable as a high-redshift QSO in a single ten minute exposure.

OSMOS has greatly benefited from previous design work for instruments built by the Imaging Sciences Laboratory at the Ohio State University Department of Astronomy.[3] Development time and expense were reduced by making use of mechanical, electrical, and software design solutions developed for the MODS spectrograph[4] and other instruments. Many of these are applications of industrial automation solutions that should have wide applicability to a large variety of other instrument projects. The command structure and user interface of OSMOS are descendants of those first written for the Ohio State Imaging Fabry-Perot Spectrometer (IFPS).[5]

Figure 1. Narrowband Hα image of NGC 4625, which has an extended UV disk. The seeing was 1.3" and the total exposure time was one hour. Several exposures during this run had image quality better than 0.9".

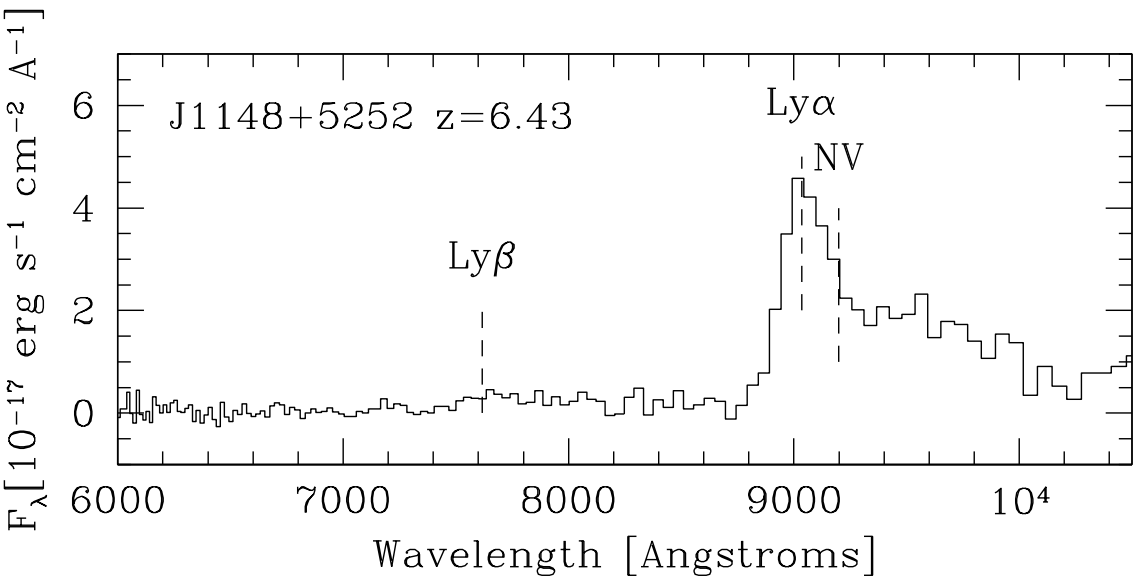

Figure 2. Spectrum of the z=6.43 QSO (z=20 mag AB) discovered by Fan et al. (2003) with the OSMOS triple prism and a 0.9" slit. The total exposure time was 40 minutes.

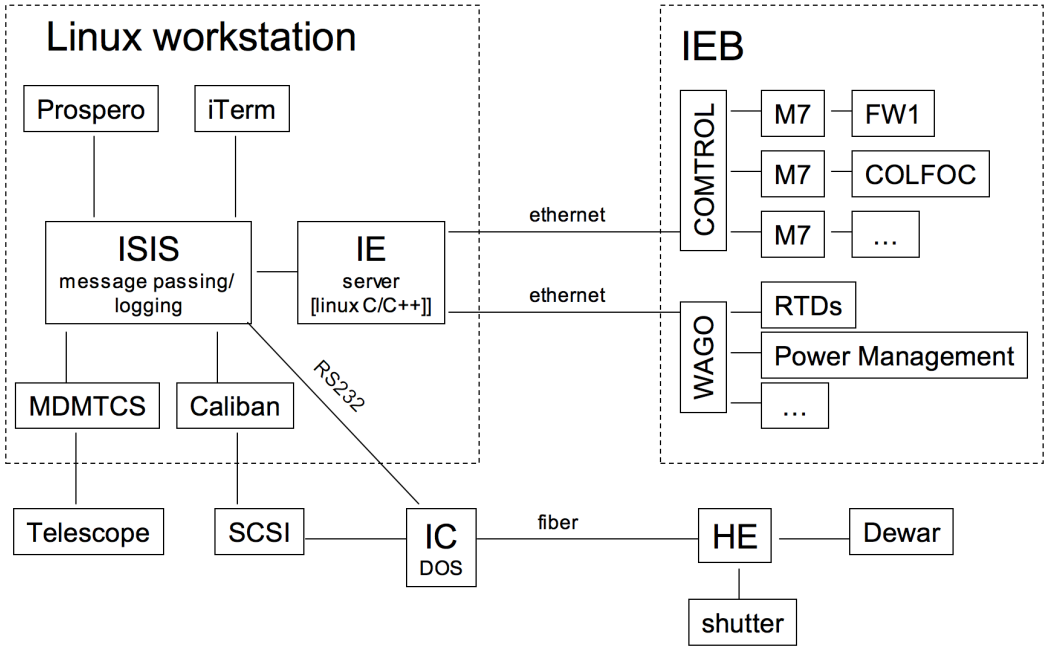

Figure 3. Block diagram of the OSMOS command structure. The dashed box on the right encloses the portion of the command structure performed by the instrument electronics box, which is mounted with the spectrograph on the telescope. The functions of the IEB include driving the mechanisms via the MicroLYNX 7 (M7) motor controllers, reading the resistance temperature detectors (RTDs), and performing power management tasks. A block diagram of the IEB is shown and explained in more detail in Fig. 4. The dashed box on the left shows the programs which run on the observer's workstation. Prospero serves as user interface and director. The iTerm is an engineering interface for the MicroLYNX motor controllers. MDMTCS is the telescope control system. Caliban, SCSI, the IC, the detector head electronics box (HE), the shutter, and the dewar are all part of the data taking system.

2. OSMOS COMMAND STRUCTURE OVERVIEW

The primary function of the instrument electronics is to run OSMOS's six mechanisms. The observer's interface is Prospero*, a program first written in 1995 to run IFPS at the Perkins Observatory 1.8m telescope. Prospero has been extensively developed since that time and is now used in OSIRIS,[6] TIFKAM,[7] ANDICAM,[8] DANDICAM, CCDS, the MDM 4K, and Y4KCam, in addition to OSMOS. It provides a single interface for CCD and instrument control, basic telescope interaction (depending on the site), and the flexibility of operating with both a command line interface and scripts.

Prospero serves as a director and translator. It takes a user command and decides whether it is meant for the CCD controller, the telescope, or the instrument, and communicates using the Ohio State ICIMACS[9] (Instrument Control and IMage ACquisition System) messaging protocol version 2.5 (IMPv2). Prospero then passes the IMPv2 command to ISIS, which logs the command and directs it to the appropriate recipient. A full overview of the OSMOS command structure can be seen in Fig. 3. Here we describe the functions controlled by the OSMOS Instrument Electronics Box, or IEB.

The primary commands sent to the IEB are those that move the mechanisms. The user issues a command in Prospero, which translates it to IMPv2 and passes it to ISIS. ISIS logs the command and passes it to the instrument electronics server (IE). The IEB contains a Comtrol serial port server that passes a move command from the IE to the appropriate MicroLYNX motor controller. The MicroLYNX interprets the command and sends the appropriate instructions to move the motor. A block diagram of the OSMOS IEB is shown in Fig. 4.

*http://www.astronomy.ohio-state.edu/~prospero/

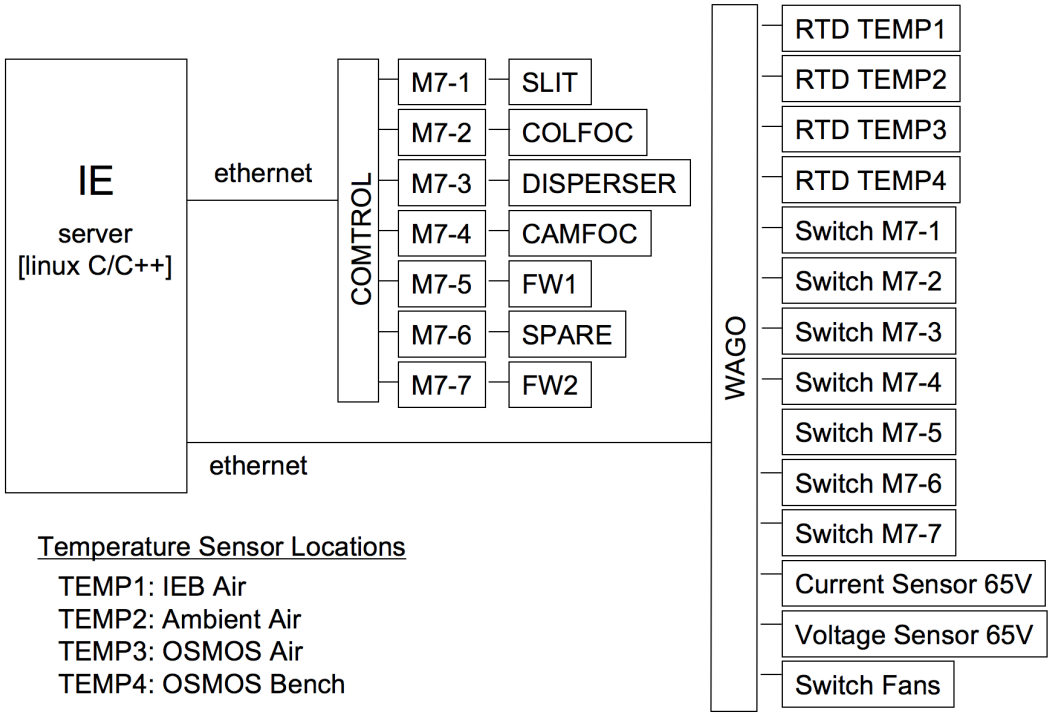

Figure 4. Block diagram of the OSMOS Instrument Electronics Box (IEB). The Comtrol is a serial port server that communicates with the MicroLYNX 7 motor controllers (M7-X). Each MicroLYNX is connected to the mechanism it controls: the slit wheel, the collimator focus, the disperser wheel, the camera focus, and the two filter wheels. There is one spare MicroLYNX to to allow for future expansion or repair. The other IEB functions are mediated by the WAGO fieldbus, including reading the four temperature sensors (RTDs), switching the fans and the individual MicroLYNX, and reading the current and voltage of the 65V unregulated power supply.

The MicroLYNX programmable motor controllers are an industrial automation solution that we have adopted for OSMOS. One of the virtues of these programmable logic controllers is that the appropriate program to operate a given mechanism is stored locally in non-volatile memory. This dramatically simplifies the commands sent to the IEB and motor controller to operate a mechanism. In addition, the simplified commands make the system more robust against communication failures than one in which detailed motor instructions are sent for each move, and make it easier to port to other control systems if it becomes necessary or desirable to do so.

3. OSMOS MECHANISMS

OSMOS has six motor-driven mechanisms. The camera and collimator focus mechanisms are linear stages. These move the camera and collimator barrels along the optical axis. The remaining four are six-position aperture wheels. These bring filters, slits, or dispersers into and out of the beam. These six mechanisms are labeled in Fig. 5, a view of the interior of OSMOS.

Many aspects of the OSMOS design benefit from development of the MODS spectrograph.[4] The wheel mechanisms are the third generation of similar filter wheels in the 12-position Buckeye Filter Wheel and in MODS. The design for the collimator tip/tilt/focus mechanism for MODS was directly repurposed for the OSMOS linear stage mechanisms. The electronics and software that drive the six mechanisms are closely related to electronics and software already developed for MODS.

The MicroLYNX motor controllers were chosen when designing MODS because of their capacity for expandable I/O. Although OSMOS does not use this expansion capability, retaining the same architecture from MODS for OSMOS substantially reduced the development time for both the electronics design and the software.

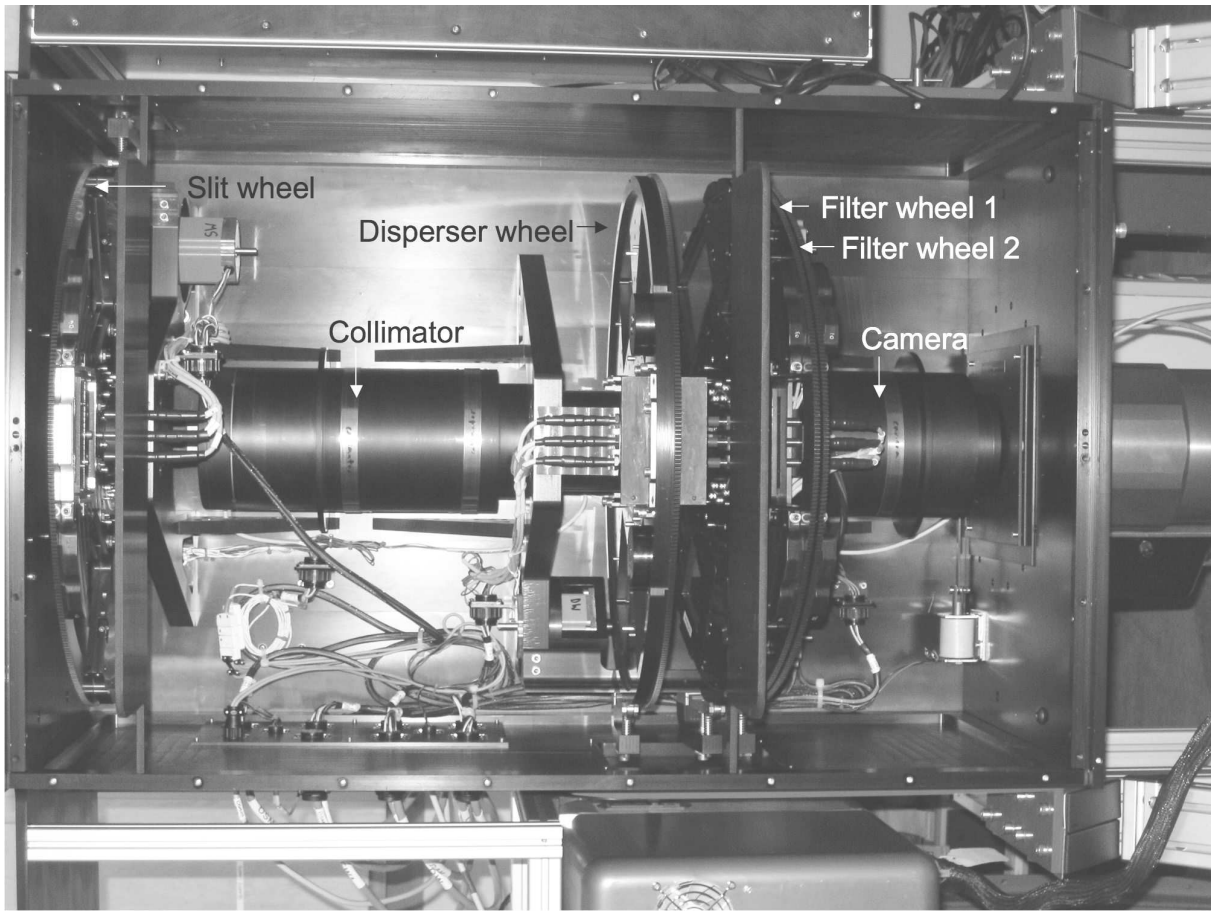

Figure 5. The interior of OSMOS. The four wheel mechanisms are labeled. The motors that drive the collimator and camera barrels are obscured by the slit wheel and the disperser and filter wheels, respectively. Light enters the instrument from the left and the detector system is to the right. Part of the IEB is visible at the top of the figure and part of the HE is visible at the bottom.

3.1 Wheel Mechanisms

The four wheel mechanisms have six apertures each. The slit wheel lies at the telescope focal surface. One aperture remains empty to allow for imaging and acquisition, and the other five can be populated with longslits or multi-object masks. The slit wheel is accessible via a hatch, so masks can be changed by the observer during the night if more than five are desired. The disperser wheel and the two filter wheels lie in the collimated beam. One aperture of the disperser wheel remains empty, like the slit wheel, to allow for imaging and acquisition. Currently two dispersers are installed, a R≈60–400 triple prism and a R≈1600 VPH grism (for a 1" slit). The two filter wheels are mounted at an angle of 8° to reduce ghost reflections. This angle is small enough to minimize the slight wavelength change for narrow-band interference filters caused by tilted filters. The filter wheels are also accessible via a hatch for easy installation and removal.

Each wheel mechanism is driven by a graphite-infused resin pinion gear that engages to the outer diameter of a bull gear bolted to the wheel assembly. The bull gear blank is a commercial gear from Trojon Gear Inc. The pinion gear is bonded to the shaft of a Superior KML062F07 motor. Each wheel turns on a custom Kaydon turntable bearing. These bearings provide two important benefits. First, they have an extremely thin profile, which is important for conserving the limited space available in the collimated beam. Second, they deflect very little ($\pm 1\mu$m) in response to force applied normal to the wheel plane, which helps to mitigate against flexure.

Each of the six wheel positions is indexed with three steel pins that encode the wheel position in binary and one pin that registers when the wheel is in a valid position. The pins are read by Pepperl+Fuchs inductive proximity sensors. Because the positions are indexed, the MicroLYNX controller does not need to keep track of what moves have been carried out in order to know the current position. Power or communications interruptions likewise do not cause loss of position information. Perhaps more importantly, use of an indexed system means that we do not need to rely on the motor position to determine the wheel position, but may instead rely on something more precise and repeatable.

The wheel is held in a given position by a mechanical detent. This detent is a bearing on a lever arm that is held against the wheel by a stiff spring to kinematically dock the wheel at that location. The surface on the wheel against which the detent rolls has six indentations corresponding to the six aperture locations. When the motor completes a move, the motor current is released and the wheel is free to move. If the detent is not resting at the center of the indentation when this happens the detent spring backdrives the wheel to the appropriate position. The radius of curvature of the base of the indentation is slightly smaller than the radius of the bearing, so that when in position the bearing rests solely on two tangent points. This makes for superb repeatability in wheel position. We have measured the repeatability to correspond to less than 1.5μm or 0.03" of image motion (less than a tenth of a pixel).

The wheels are held in position by the torque provided by the detent. The detent was designed to provide approximately three times the combination of other, parasitic torques. One of these is the motor cogging torque, or the torque exerted by the motor when the current is off, which is scaled by the gear ratio. Another is the drag torque of the wheel, in this case probably dominated by the friction of the central bearing. The last is any torque caused by an asymmetrically loaded or unbalanced wheel.

A motion is initiated in Prospero by specifying which of these six positions one wishes to move into the beam. This is communicated by Prospero via ISIS to the IE, which passes the command on through the serial port server to the appropriate MicroLYNX motor controller. The motor controller has the program for the mechanism it controls in non-volatile memory. When it receives a command to move, the program directs it to first read the sensors to check the current position of the wheel. It then calculates how many positions to move and in which direction and sends the instructions for that move to the motor. The motor commands are constructed so that each move is composed of a series of one-position moves. This enhances repeatability by preventing stalling over the intervening detent indentations. At the end of the move, the sensors are read again to confirm that it has arrived in the correct position.

If the wheel ever ends out of position, the final sensor read will not register an in-position bit, and Prospero will return an error to the user stating that the wheel ended out of position and must be reset. Resetting the mechanism steps the motor slowly through one move, repeatedly reading the sensors until the wheel registers

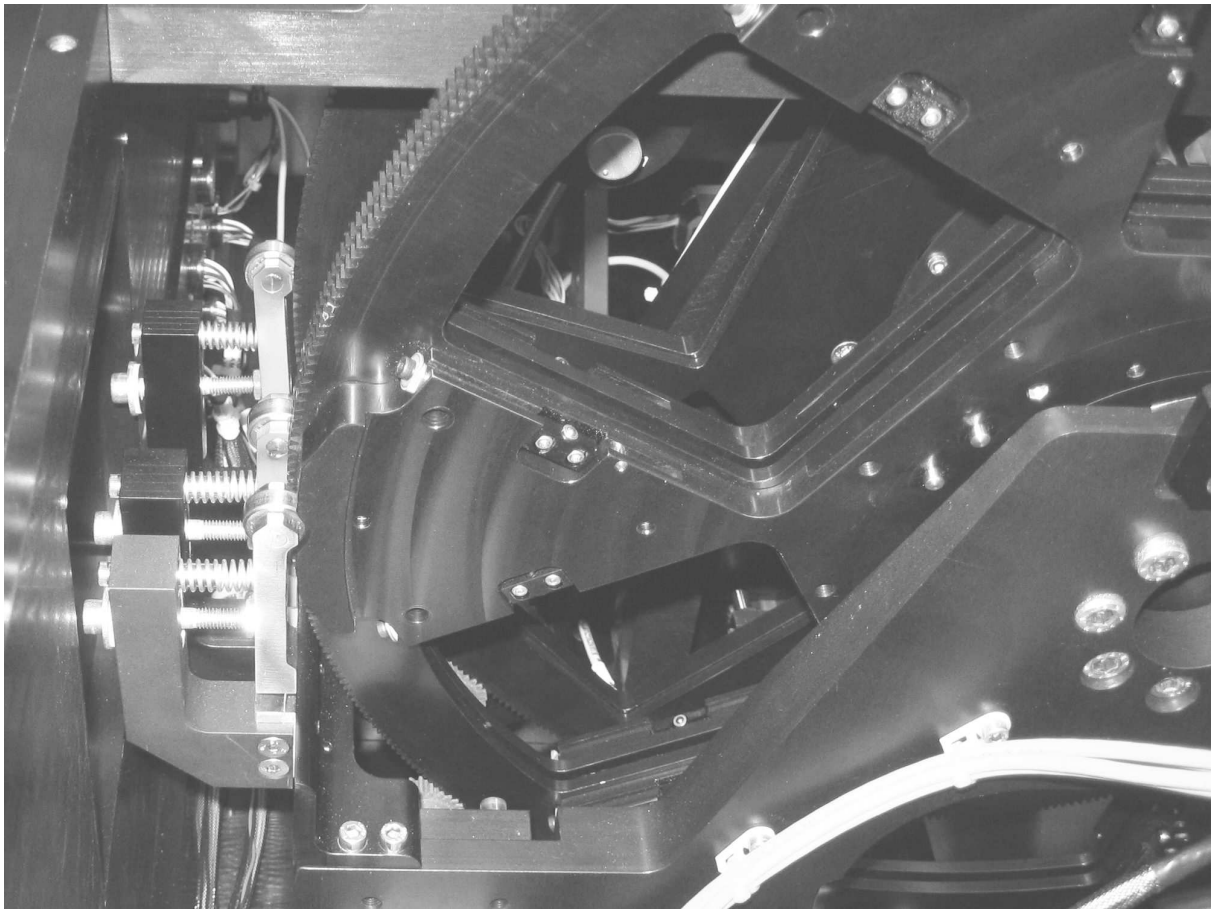

Figure 6. A closeup of filter wheel 2. The detent is the structure on the left side. Behind it are the detents for filter wheel 1 and the disperser wheel.

that it is in a valid position. Prospero then reports to the user the current position, and the original move command can be reissued.

One step of the stepper motor corresponds to 1/200th of a rotation of the motor shaft. The move length to change wheel position is set by this, by the sub-precision to which we have decided to set the motor controller, by the gear ratio, and by the number of positions on the wheel. The microstep size we have set is 1/10, the gear ratio is 19, and the number of positions on each wheel is six. Nominally, then, there are 6333 motor steps (or rather, microsteps) between wheel positions. The imprecision imposed by a discrete number of motor steps leads to an imprecision of positioning of slightly less than 2'. Considering microsteps instead, that imprecision drops to 11". At the end of the move, however, the current to the motor is stopped, releasing the mechanism to settle into the position dictated by the detent.

3.2 Linear Stage Mechanisms

There are two linear stage mechanisms that move the collimator or camera along the optical axis so the two focal surfaces correspond to the slit surface and the detector surface, respectively. Each linear stage mechanism is driven by an Applied Motion HT 17-075-D motor, which is coupled to a linear stage with a 6mm pitch by a 1/100 harmonic reducer.

The linear stages are not indexed or encoded mechanisms. Each has two proximity sensors which define the limits of the range of motion of the stage. The stage position is measured in microns from the home position, which is the sensor assert location of the clockwise limit. The stage of course spends most of its time at the

focal position, which is in the middle of the range, in the region where neither of the sensors is activated. The position is defined relative to the home position and is tracked by the MicroLYNX based on the number of motor turns that have been carried out since the last time the mechanism encountered the home limit. Because of this, a power cycle means that the mechanism will wake up with no sensor asserted and will have lost its relative position information. If an observer wishes to move the camera or the collimator after a power cycle, he or she will have to reset the mechanism first. This reset takes approximately ten seconds.

When the instrument is pointed towards the zenith, the weight of the optics is parallel to the screw of the linear stage. Like the wheel mechanisms, the linear stages do not maintain their position by active immobilization. Once a motion is complete, the motors turn off rather than maintain an idle current. Unlike the wheel mechanisms, the linear stages are not held in place by a separate mechanical assembly like the detent. The camera and collimator remain immobile essentially because the torque provided by the weight of the optics against the pitch angle is less than the stabilization provided by the motor cogging torque, which is effectively amplified by the harmonic reducer. The specifics are slightly more complicated, involving the screw pitch of the linear stage and the efficiency of the harmonic reducer and of the linear stage. To an order of magnitude, however, the resistance is simply the cogging torque multiplied by the inverse of the 1/100 ratio of the harmonic reducer.

The linear stages are capable of much more precise positioning than needed. The stepper motor has 200 steps per revolution and we have it set to ten microsteps per step. The harmonic reducer is a factor of 100, and the screw pitch is 6 mm. One step of the motor moves the optic 0.30μm. We have set the MicroLYNX so positions are defined in microns rather than steps, and we specify moves to one micron. The position is defined relative to a sensor assert position, and its precision is limited by this. We measure the repeatability by repeatedly driving the stage into the counterclockwise limit and calculating the rms of where the limit asserts. This gives a precision of approximately 1.5μm. This is orders of magnitude smaller than the depth of focus, which we measure to be approximately 100μm. The overengineered precision of the camera and collimator focus mechanisms is a result of repurposing the collimator tip/tilt/focus mechanism designed for MODS. This efficiency reduced the development time and expense for OSMOS by more than the extra expense of the overly capable components.

4. OTHER IEB FUNCTIONS

Although the primary function of the IEB is to drive the six mechanisms, it performs several other monitoring and power switching functions. We use a WAGO modular fieldbus system to do many of these tasks.

4.1 Temperature Measurement and Control

The IEB includes four resistance temperature detectors (or RTDs) that are read via a pair of WAGO modules. One sensor measures the temperature of the optical bench, one measures the air temperature inside the instrument, one measures the temperature of the ambient air in the dome, and one measures the temperature inside the IEB. These four temperatures are displayed on the instrument status window. They are also recorded in the image headers. The temperature data during the commissioning run is shown in Fig. 7. The IEB temperature is consistently about 3–4° C above the dome ambient temperature. The instrument temperature is also a little above ambient, and tends to approach ambient over the course of the night. The OSMOS interior air temperature tracks the optical bench temperature closely, so it is left out of the figures for clarity. Fig. 8 overplots the temperature relative to the ambient temperature for all nights of the commissioning run to see whether this tendency is a consistent trend.

The IEB has a circulation fan and an exhaust fan. These are wired through the WAGO to allow them to be switched on and off individually, although they are set to run constantly in normal operation. As noted above, the exhaust air that the IEB vents into the dome is 3–4° C above ambient. The exhaust temperature of the Head Electronics Box of the 4K detector that will usually be used with OSMOS has not yet been measured, but direct comparison shows the OSMOS IEB exhaust temperature is much lower.

The major heat sources in the IEB are the seven MicroLYNX motor controllers and the 65V power supply. We provide power switching of each MicroLYNX through a WAGO module, but the default is to have them all turned on. We do not include a power switching capability for the power supply. The IEB consumes ∼90 W at rest. When mechanisms are running, that temporarily rises ∼30 W.

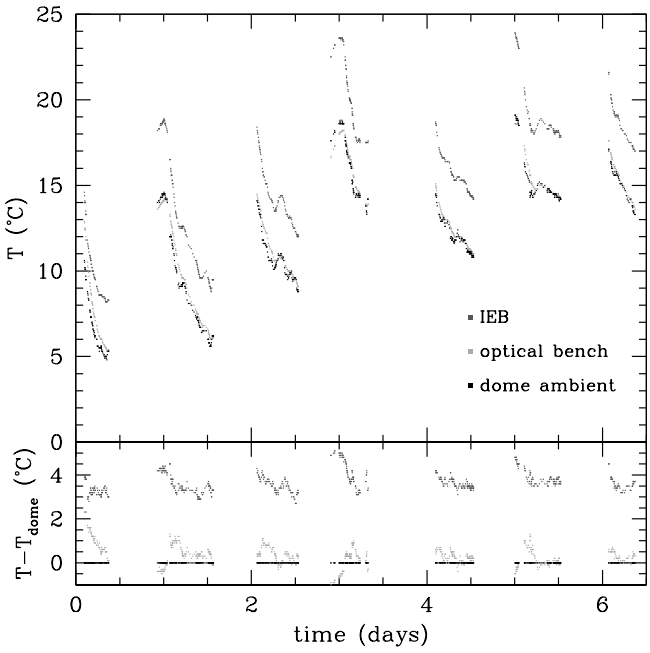

Figure 7. The top panel plots the absolute temperatures measured by three of the RTDs over the week of OSMOS on-sky commissioning in April 2010. The lower panel plots these temperatures relative to the dome ambient temperature. The relative temperatures are fairly consistent from night to night, even though the temperature at the beginning of the night varied approximately ten degrees during the week. There is some suggestion of a nightly trend as the OSMOS interior temperature (light grey) approaches the dome ambient temperature (black), while the IEB temperature (dark grey) settles fairly quickly to an equilibrium offset of 3–4° C. The OSMOS interior air temperature tracks the optical bench temperature closely, so it is left out of the figure to enhance clarity.

The primary reason the instrument itself has a temperature above ambient during much of the night is that it is in thermal contact with the telescope. Beyond that, the major source of heat inside the instrument is the minimal amount of heat released from friction when the mechanisms are moved.

4.2 Power Management

Through the WAGO we monitor the current and voltage of the unregulated 65V power supply we use to power the MicroLYNX. The voltage is scaled down by a resistor to the range measurable by the WAGO. The current sensor is constructed from a commercial Hall Effect sensor.

ACKNOWLEDGMENTS

OSMOS has been generously funded by the National Science Foundation (AST-0705170) and the Center for Cosmology and AstroParticle Physics at The Ohio State University. Additional support has also been provided by the Department of Astronomy at The Ohio State University and the Department of Physics and Astronomy at Ohio University.

REFERENCES

[1] Martini, P. *Publ. Astron. Soc. Pacific* , in preparation (2010).

[2] Fan, X. et al., "A Survey of z>5.7 Quasars in the Sloan Digital Sky Survey. II. Discovery of Three Additional Quasars at z>6," *Astron. J.* **125**, 1649–1659 (Apr. 2003).

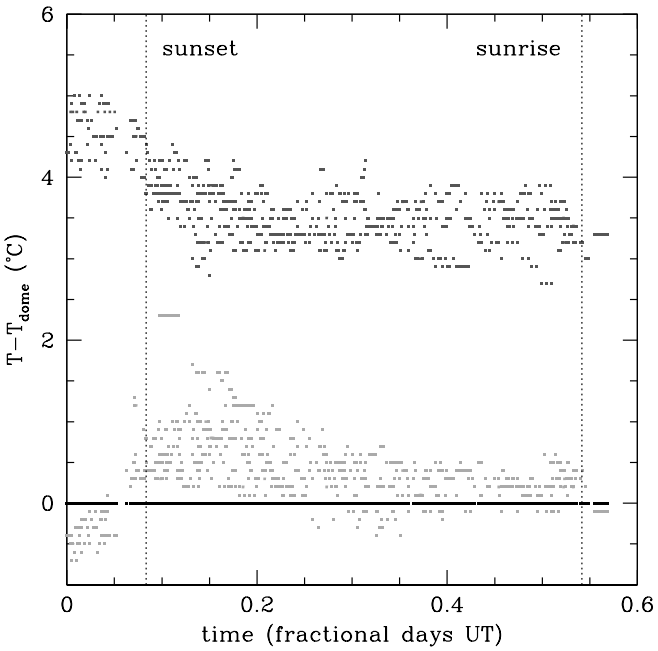

Figure 8. Relative temperatures from all nights are overplotted to demonstrate the night-to-night consistency of the trend shown in Fig. 7 Although there are overall trends, the scatter from night to night is considerable. On average, it appears to take approximately five hours for the instrument temperature to equilibrate to approximately the dome ambient temperature, but only about two hours for the IEB temperature to equilibrate to about 3.5° above ambient. The shades are the same as in Fig. 7.

[3] Atwood, B. et al., "Ohio State University Imaging Sciences Laboratory (ISL)," in [*Society of Photo-Optical Instrumentation Engineers (SPIE) Conference Series*], A. M. Fowler, ed., *Society of Photo-Optical Instrumentation Engineers (SPIE) Conference Series* **3354**, 777–781 (Aug. 1998).

[4] Pogge, R. W., et al., "The multi-object double spectrographs for the Large Binocular Telescope," in [*Society of Photo-Optical Instrumentation Engineers (SPIE) Conference Series*], *Society of Photo-Optical Instrumentation Engineers (SPIE) Conference Series* **6269** (July 2006).

[5] Pogge, R. W., Atwood, B., Byard, P. L., O'Brien, T. P., Peterson, B. M., Lame, N. J., and Baldwin, J. A., "The Ohio State Imaging Fabry-Perot Spectrometer (IFPS)," *Publ. Astron. Soc. Pacific* **107**, 1226 (Dec. 1995).

[6] DePoy, D. L., Atwood, B., Byard, P. L., Frogel, J., and O'Brien, T. P., "Ohio State Infrared Imager/Spectrometer (OSIRIS)," in [*Society of Photo-Optical Instrumentation Engineers (SPIE) Conference Series*], A. M. Fowler, ed., *Society of Photo-Optical Instrumentation Engineers (SPIE) Conference Series* **1946**, 667–672 (Oct. 1993).

[7] Pogge, R. W. et al., "MDM/Ohio State/ALADDIN infrared camera (MOSAIC)," in [*Society of Photo-Optical Instrumentation Engineers (SPIE) Conference Series*], A. M. Fowler, ed., *Society of Photo-Optical Instrumentation Engineers (SPIE) Conference Series* **3354**, 414–418 (Aug. 1998).

[8] DePoy, D. L. et al., "A Novel Double Imaging Camera (ANDICAM)," in [*Society of Photo-Optical Instrumentation Engineers (SPIE) Conference Series*], M. Iye & A. F. M. Moorwood, ed., *Society of Photo-Optical Instrumentation Engineers (SPIE) Conference Series* **4841**, 827–838 (Mar. 2003).

[9] Atwood, B., Mason, J. A., Duemmel, K. R., O'Brien, T. P., Pogge, R. W., Pappalardo, D., and Hartung, B., "ICIMACS: the Ohio State Instrument Control and Image Acquisition System," in [*Society of Photo-Optical Instrumentation Engineers (SPIE) Conference Series*], S. D'Odorico, ed., *Society of Photo-Optical Instrumentation Engineers (SPIE) Conference Series* **3355**, 560–564 (July 1998).